Activation of Superficial and Deep Finger Flexors through Transcutaneous Nerve Stimulation

Henry Shin, Marwan A. Hawari, Xiaogang Hu

Abstract— Objective: **Functional electrical stimulation (FES) is a common technique to elicit muscle contraction and help improve muscle strength. Traditional FES over the muscle belly typically only activates superficial muscle regions. In the case of hand FES, this prevents the activation of the deeper flexor muscles which control the distal finger joints. Here, we evaluated whether an alternative transcutaneous nerve-bundle stimulation approach can activate both superficial and deep extrinsic finger flexors using a high-density stimulation grid.** *Methods:* **Transverse ultrasound of the forearm muscles was used to obtain cross-sectional images of the underlying finger flexors during stimulated finger flexions and kinematically-matched voluntary motions. Finger kinematics were recorded, and an image registration method was used to capture the large deformation of the muscle regions during each flexion. This deformation was used as a surrogate measure of the contraction of muscle tissue, and the regions of expanding tissue can identify activated muscles.** *Results:* **The nerve-bundle stimulation elicited contractions in the superficial and deep finger flexors. Both separate and concurrent activation of these two muscles were observed. Joint kinematics of the fingers also matched the expected regions of muscle contractions.** *Conclusions:* **Our results showed that the nerve-bundle stimulation technique can activate the deep extrinsic finger flexors, which are typically not accessible via traditional surface FES.** *Significance:* **Our nerve-bundle stimulation method enables us to produce the full range of motion of different joints necessary for various functional grasps, which could benefit future neuroprosthetic applications.**

Index Terms— **Functional Electrical Stimulation. Nerve Stimulation, Muscle Activation, Ultrasound Image Deformation**

I. Introduction

The restoration of hand function and the ability to perform activities of daily living are often ranked as the highest priorities for individuals following a neurological injury such as stroke [1] or spinal cord injury [2]. Functional Electrical Stimulation (FES) is widely used for the restoration of hand muscle strength and object manipulation in these clinical populations [3]–[6]. FES typically involves electrodes placed on the skin directly over the muscle belly that produces the desired movements. For conventional surface stimulation methods, the muscles that are closer to the skin surface are preferentially activated over other deeper muscles [7]–[9]. Therefore, it is difficult to activate important hand muscles such as the flexor digitorum profundus (FDP) which lies deeper beneath the surface. For example, FES can activate the flexor digitorum superficialis (FDS) muscle, which mainly leads to the flexion of the proximal interphalangeal (PIP) joints [10]. Stimulation of the intrinsic palmar lumbricals and interossei using additional electrodes can enable greater metacarpophalangeal (MCP) joint flexion [11], but activation of the FDP for distal interphalangeal (DIP) joint flexion is typically not achievable [12]. Without the activation of all joints, conventional hand FES may result in incomplete grasp patterns and finger prehension, which may lead to inadequate functional restoration.

As an alternative approach to activate the muscles at the motor points, invasive implantable electrodes with a direct interface to the peripheral nerve bundles have also been used for FES [13], [14]. For example, cuff electrodes or penetrating electrode arrays are implanted to the peripheral nerve bundles innervating the targeted muscles. Stimuli delivered to nerve fibers can activate specific muscles to elicit precise finger movements. Besides clinical applications, nerve bundle stimulation is commonly used in research settings to evaluate muscle activation through direct motor nerve activation or through reflex activation [3]. Without the invasive implantation procedure, electrical stimulation can also be delivered to a proximal location where the corresponding nerves of the desired muscles are locations more superficially [15], [16], which can preferentially recruit the reflex pathways. In the case of the finger flexors, the median and ulnar nerve bundles can be targeted for stimulation from the medial side of the upper arm. These two nerves innervate both the intrinsic and extrinsic flexor muscles of different fingers. The median nerve innervates flexor muscles of the index and middle fingers and partly the ring finger, and the ulnar nerve innervates flexor muscles of the little finger and partly the ring finger. Several studies have shown that stimulation of the peripheral nerve bundles can be used to generate a variety of single and multi-finger grasp patterns [17]–[20], which span all the joints of the hand. In particular, the kinematic results of this stimulation method demonstrated the feasibility of flexing the DIP joints [17]. Although DIP flexion is mainly controlled by the FDP muscle, it is not well understood from the kinematics alone whether the DIP joint was actively flexed by the activation of the FDP, or moved indirectly by the contraction of other muscles. The validation of the active contraction of the FDP muscles due to proximal nerve stimulation is an important exploration of the method, which

Shin, Hawari, and Hu are with the Joint Department of Biomedical Engineering at University of North Carolina-Chapel Hill and NC State University (correspondence e-mail: xiaogang@unc.edu). Shin is now with Ripple LLC, Salt Lake City, UT 84106 USA (e-mail: hhshin@ncsu.edu).

supports its utility as a FES approach.

The detection of muscle activation is most commonly investigated using electromyography (EMG) at the surface of the skin to record the changes of electrical potential caused by the excitation-contraction coupling of underlying skeletal muscles [21]. However, non-invasive EMG approaches are also typically limited to the superficial muscles and cannot discriminate between signals from superficial or deep sources. Alternatively, intramuscular EMG has high spatial specificity, but can be difficult for routine practice to target the desired muscles without prerequisite expertise [22]. Rather than measuring electrical signals, another option for detecting muscle contraction is to use imaging techniques to capture the changes of muscle morphology [23], [24]. Ultrasound is a commonly used imaging modality due to its low-cost, fast, and convenient ability to obtain images of muscle tissues during contraction [25]. Ultrasound images of muscles are recorded either longitudinally along the length of a single targeted muscle or transversely to the limb so that a cross-section of multiple muscles can be imaged. Transverse ultrasound of the forearm has been commonly used for finger motion recognition and classification due to its ability to capture the contractions of a number of muscles or muscle compartments simultaneously [25]–[27].

Accordingly, the objective of the current study was to use transverse ultrasound imaging to investigate whether the nerve-bundle stimulation induced activation of FDS and FDP muscles. To capture the specific muscle contraction, we used muscle deformation to identify activation of the forearm muscles during finger flexion. Prior to this study, we also performed intramuscular recordings as a preliminary validation of the ultrasound muscle deformation as a surrogate measure of muscle activation [28]. The transverse forearm ultrasound was recorded during stimulated flexions and kinematically-matched voluntary flexions. Our results revealed a significant correlation in the muscle deformation locations between the stimulated and voluntary motions. We were able to show the activation of muscles at two distinguishable depths associated with the FDS and FDP muscles, which corresponded to the finger joint kinematics. This selective or concurrent activation of the extrinsic flexor muscles supports the utility and future development of the proximal nerve-bundle stimulation method as an alternative to conventional FES techniques.

II. METHODS

A. Subjects

In this study, 12 intact subjects (10 males, 2 females, 19-35 years of age) without any known neurological disorders were recruited. Before experimentation, all subjects gave informed consent with protocols approved by the Institutional Review Board of the University of North Carolina at Chapel Hill.

B. Experimental Setup

1) Electrical Stimulation

After cleaning the skin with alcohol wipes, a 2×8 grid of gel electrodes, approximately 1 cm in diameter (NeuroPlus Disposable Medical Electrodes, Vermed, Inc.), were placed on the subject's right upper arm near the short head of the biceps brachii on the medial side. This placement (Figure 1), was chosen for its superficial proximity to the median and ulnar nerve bundles [29], [30]. The 16 electrodes were connected through a switch matrix (34904A, Agilent Technologies), which allowed any two electrodes to be connected to the anode and cathode of a bipolar programmable stimulator (STG4008; Multichannel Systems, Reutlingen, Germany). The electrodes were secured in place using a custom vice that applied pressure over the electrode array into the subject's upper arm. Stimulation was controlled using a custom MATLAB (version 2016b, MathWorks Inc) user-interface. All stimulation trains were designed using charge-balanced biphasic pulses of 500 μs pulse width at 30 Hz. Current amplitude was modulated in the experiment to induce muscle contraction at different pairs of electrodes

2) Finger Motion Tracking

Subject's finger kinematics were recorded using an 8-camera motion tracking system (Optitrack; Natural Point, Inc). Five 6 mm IR-reflective markers were placed on each of the fingers of the subject's right hand. Markers were adhered to the skin immediately proximal to each of the 3 joints of each finger with 2 additional references placed on the fingernail and over the metacarpal bone. A 4-marker rigid body was placed at the wrist to orient the rotation of the forearm. The 3D positions of all the markers were recorded in 120 Hz using motion capture software (Motive; Natural Point, Inc).

3) Ultrasound Recordings

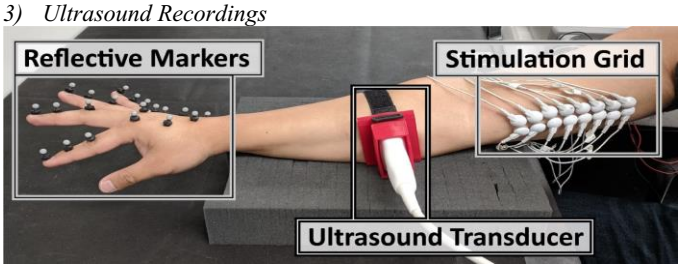

Figure 1: Experimental Setup. Reflective markers were placed on the hand to track finger motions and ultrasound was recorded along the forearm to image the changes in muscle tissue with contraction. A stimulation grid was placed along the medial side of the upper arm. Note: the hand was rotated for the purpose of the picture and does not represent the normal neutral position.

The transverse cross-section of muscle contraction was recorded in all subjects using a clinical Doppler ultrasound system (S2, SonoScape Medical Corp.) with a 5-10 MHz linear array transducer (L741, SonoScape Medical Corp.), which was inserted into a custom 3D printed holster. As seen in Figure 1, the ultrasound probe and holster were then secured on the subject's arm at a distance 25% down the length of the forearm from the cubital fossa to the wrist. A concentric Velcro strap was used to hold the holster at this location for the entire duration of the experiment. This location was chosen because it contains the largest volume of the extrinsic finger flexor muscles. All ultrasound images were directly recorded at a sampling rate of 54 frame per second (fps), and subsequently exported to MATLAB in sets of 46×46 mm image frames.

This article has been accepted for publication in a future issue of this journal, but has not been fully edited. Content may change prior to final publication. Citation information: DOI 10.1109/JBHI.2020.3041669, IEEE Journal of Biomedical and Health Informatics

C. Experimental Procedure

All subjects were seated comfortably in a chair with their right arm resting in front of them on foam blocks. The subject's hand was oriented so that their forearm was in a neutral position. After the experimental setup was completed, the stimulation electrode array was used to identify unique stimulated motions which ideally induced single finger motions in only the PIP or DIP joints. Prior to the main experiment, we first performed an electrode search procedure to identify the viable electrode pairs that could elicit the desired joint motions. During this process, the electrode pairs that can induce skin discomfort were excluded from further use. We also excluded electrodes that could induce pain or uncomfortable feelings during the experiment. A custom MATLAB GUI was used to deliver stimulation pulse trains of 1 second duration to any pair of electrodes in the stimulation array. Typically starting at 2-3 mA pulses, random pairs of electrodes were stimulated, and the fingers were observed for any distinguishable movements. Subjects were then asked to voluntarily return to the same pre-stimulation baseline position after each stimulation. This was repeated across the entire electrode grid until at least two distinct motions were found in different sets of fingers. When possible, the chosen stimulation locations elicited one proximal motion of mostly PIP joints, and one distal motion of mostly the DIP joints. For these selected stimulation locations, the amplitude was increased in 0.1 mA increments until the strongest level of activation of the specified motion was possible without additional recruitment of adjacent fingers or joints.

A custom triggering circuit was built to allow synchronization between the beginning of the electrical stimulation, ultrasound recording, optical motion capture. Separate trials of 16 seconds were recorded for each stimulated or voluntary-matched experimental condition. For a single stimulated trial, the stimulation train was programmed with 1 second of starting delay, and then 5 repetitions of 1 second of stimulation and 2 seconds of rest. During every rest period, the subjects were asked to extend their fingers back to the neutral baseline position and fully relax before the next stimulation. The stimulated motion was repeated for a total of three trials to obtain a total set of 15 stimulated flexion events. Following the set of stimulated movements, three matched-voluntary motion trials were also recorded for a total duration of 16 seconds each. Before each voluntary contraction, the subjects were first given visual displays of the stimulation evoked joint motions, and the subjects were then asked to replicate the displayed joint motions as a practice. During voluntary contraction trials, visual feedback of the joint motion was provided as a guidance for voluntary motions. In addition, a 1 Hz metronome was used to help the subjects to time the flexion and extension of the voluntary movement on alternating beats. This resulted in 6~7 flexions per trial or 18~21 total flexions. This overall procedure was repeated for each of the stimulated and corresponding matched-voluntary motions, resulting in a minimum of 12 ultrasound and motion capture recordings per subject with two sets of motions.

D. Data Processing

1) Joint Angle Kinematics

The location and rotation of the wrist rigid body was used as the origin of the marker data so that all the motions were in a similar starting orientation. The angle of each of the MCP, PIP, and DIP joints were calculated. The angle was defined so that a straight, neutral finger position was 0° and flexion from this posture resulted in a negative angle. The resultant joint kinematic data were then used to obtain the timing of the start and end of every voluntary flexion movement. The angular

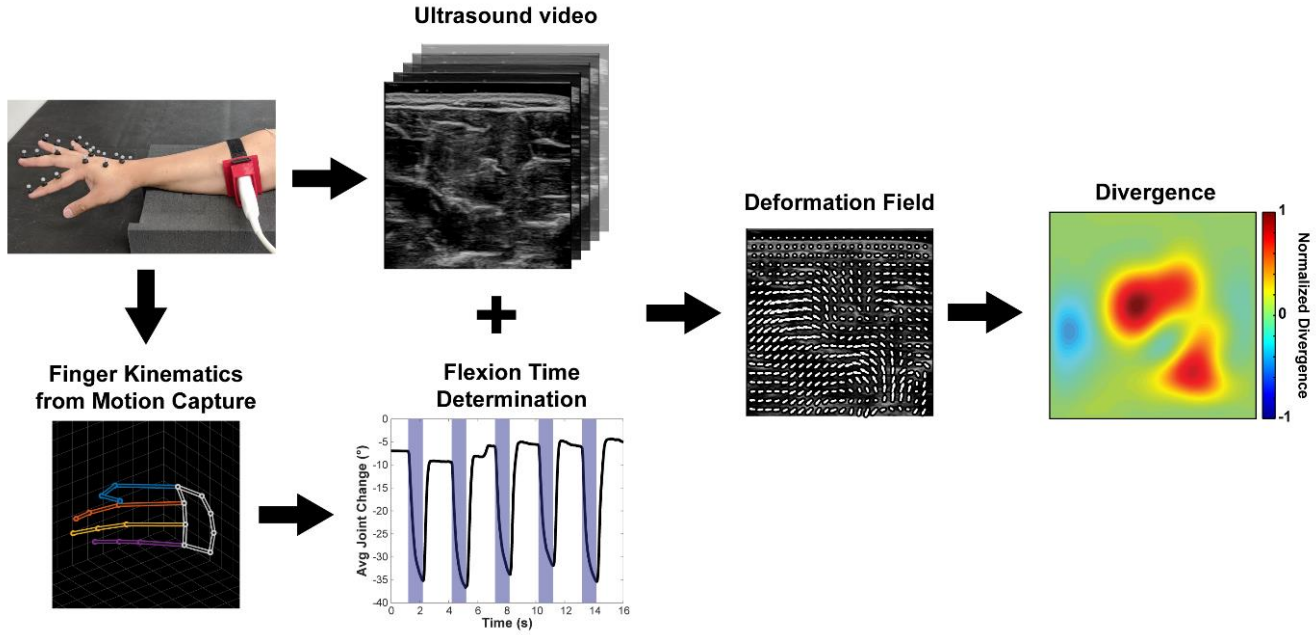

Figure 2: Overview of Data Processing. For every stimulated or voluntary motion, the finger kinematics and the ultrasound images were obtained from a synchronized start time. The start and end flexion times were determined for each flexion event, and the deformation of the ultrasound image between these times was calculated. An average of the deformation fields from all the flexion events was then used to calculate the divergence. Numerically this signifies the sources and sinks from the previous vector field and is an indication of the regions of concentric expansion of tissue.

This article has been accepted for publication in a future issue of this journal, but has not been fully edited. Content may change prior to final publication. Citation information: DOI 10.1109/JBHI.2020.3041669, IEEE Journal of Biomedical and Health Informatics

displacement ($\theta(t)$) of all the joints were averaged for a single trial, and the derivative of this average ($\dot{\theta}(t)$) was calculated to find the time at which the overall joint motion began flexion ($\dot{\theta}(t) \leq -0.1\ ^\circ/s$) and subsequently stopped before returning to neutral position. The start and end times of the stimulated flexion movements were taken directly from the known times of each 1s stimulation train. These flexion times were then used to extract the ultrasound image frames which matched the movement times.

2) Ultrasound Deformation and Divergence Calculation

For every movement, the ultrasound image deformation between the start and end of the flexion was used as a surrogate measurement of muscle contraction. A demons image registration algorithm [31] was used to quantify the pixel-wise deformation between pairs of ultrasound images. Specifically, the diffeomorphic demons algorithm [32] implemented in MATLAB (imregdemons()) was utilized to obtain a differentiable and invertible displacement vector field which prevents physically impossible transformations from occurring, such as a folding of the image. These 2D vector fields represent the estimated "diffusion" or movement of individual pixels from one image to another, and has been previously applied during finger movements to detect regions of muscle tissue contraction [26].

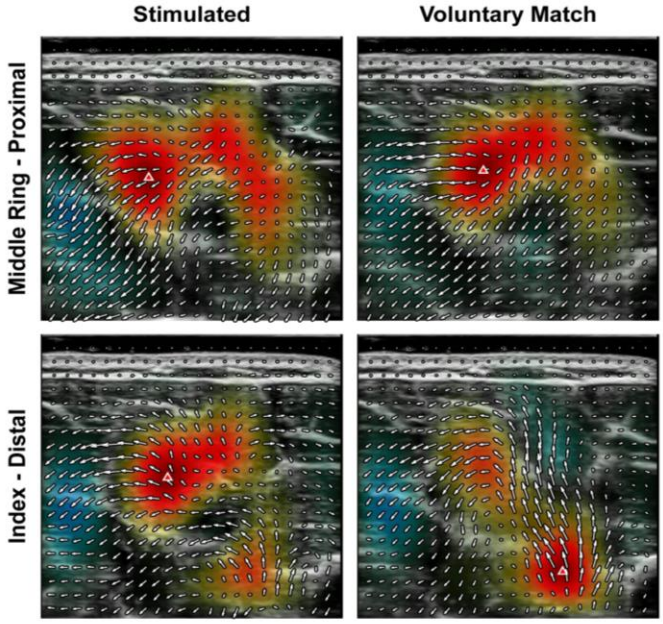

Figure 3: Sample Ultrasound Deformation and Divergence for a Single Subject. Each image represents the total image deformation and divergence from each stimulated location and its matched-voluntary movement. The red triangles indicate the precise location of the maximum divergence value. Rows represent a single stimulated motion pattern, and the columns represent the movement condition. Of note is the bottom row which also contains an example of divergence maps with two distinct local maxima.

The displacement field from any image registration can be considered as a mapping function ($\vec{s}$) of each pixel in the moving image (I_M) to the reference or fixed image (I_F). If the image registration algorithm is accurate, a mapping function applied to the moving image is approximately equal to its fixed image ($\vec{s}(I_M) \cong I_F$). In previous uses of image registration for muscle ultrasound [26], only the image frames from the start and end of the motion were used for the deformation calculation. In the current study, 5 equally spaced images between the start and end of each flexion were extracted from each flexion motion ($I_1, \ldots, I_5$). These smaller time steps were used to isolate smaller regional deformations of ultrasound through the flexion movement. The earlier image frame was considered the fixed image between each subsequent image pair, and the deformation of each step was calculated between adjacent times.

$$I_1 \underset{s_1}{\rightarrow} I_2 \underset{s_2}{\rightarrow} I_3 \underset{s_3}{\rightarrow} I_4 \underset{s_4}{\rightarrow} I_5$$

With multiple sequential steps, each mapping function only represents the deformation that occurs between steps relative to the fixed image of the pair. (e.g. s_1 represents the deformation of I_1 onto I_2 with respect to I_1). By applying subsequent mapping functions recursively, it is possible to transform a deformation step to the reference coordinates of a previous image.

$$\Delta_{2\rightarrow 3,I_1} = s_1(s_2)$$
$$\Delta_{3\rightarrow 4,I_1} = s_1(s_2(s_3))$$
$$\Delta_{4\rightarrow 5,I_1} = s_1(s_2(s_3(s_4)))$$

A summation of these smaller deformations then represent the total deformation ($\vec{F}$) that occurs between the starting and ending image frames of a single flexion motion.

$$\vec{F}_{1\rightarrow 5} = s_1 + s_1(s_2) + s_1(s_2(s_3)) + s_1(s_2(s_3(s_4)))$$

For each experimental condition, a single average ultrasound image deformation ($\vec{F}_{avg}$) was obtained from all the individual flexion events. The divergence of the deformation field was then calculated to reduce the dimensionality of the deformation while also better quantifying the regions of concentric expansion due to muscle contraction.

$$\text{div}\,\vec{F}_{\text{avg}} = \nabla \cdot \vec{F}_{\text{avg}} = \frac{\partial F_x}{\partial x} + \frac{\partial F_y}{\partial y}$$

The divergence of a vector field measures the flux or change of the field, and can be related to the magnitude of a source or sink in a fluid flow. The divergence of the deformation in this case represents the relative expansion or contraction of the tissue at each pixel location. Figure 2 shows an overview of the data processing steps. Figure 3 shows a sample set of voluntary and stimulated divergence of the muscle deformation from a single subject. The sample starting ultrasound image frame is overlaid with a corresponding deformation field and its pseudo-color divergence result. The x-y coordinate location of the maximum divergence was obtained from all movement sets as a summary measure of the muscle contraction center.

3) Proximal/Distal Joint Movement Categorization

To categorize and label the elicited movements (proximal vs. distal joints), the previously obtained flexion times were also used to isolate the average flexion angular displacement of all the individual joints for each set of movements. These joint angles were used to calculate the relative difference between proximal and distal activation at each finger.

$$PIP{:}\,DIP\ Relative\ Difference = \frac{\theta_{PIP} - \theta_{DIP}}{\theta_{PIP} + \theta_{DIP}}$$

This article has been accepted for publication in a future issue of this journal, but has not been fully edited. Content may change prior to final publication. Citation information: DOI 10.1109/JBHI.2020.3041669, IEEE Journal of Biomedical and Health Informatics

This relative difference was then weighted by the relative total flexion of each finger ($w_{finger} = \frac{\sum\theta_{finger}}{\sum\theta_{All}}$). The weighted average across all four fingers was used to categorize movements as either a more proximal finger joint motion (P:D>0) vs a more distal one (P:D<0). Relative differences close to 0 also suggest movement of both joints in a similar range. This approach has been validated using intramuscular recordings and voluntary activation to ensure that the divergence of deformation represented muscle activation rather than muscle passive movement [28].

E. Data Analysis

The Pearson's correlation coefficient (r_{xy}) between the stimulated and matched-voluntary flexion angle displacement across all the joints (n=12) was calculated as a measure of correctly matched finger movement. Additionally, the similarity between the stimulated and matched-voluntary ultrasound was compared using the 2D correlation between the paired divergence maps.

motions besides the single joint (proximal or distal) motions. In one subject, three distinct motions could be induced, and an extra set of data was obtained.

Figure 4 shows a sample of the paired joint kinematic data, as well as a histogram of all the correlation coefficients across different trials. Among the 12 joints, a correlation coefficient above 0.576 is significantly different ($\alpha = 0.05$) from 0. Only three motion sets did not meet this criterion, demonstrating that most stimulated motions (19 of 22) were successfully matched during the subsequent voluntary motion trials. Additionally, the distribution of the 2D correlation coefficients between the ultrasound divergences was also calculated (Figure 4B). Most of these correlation values were above 0.6, indicating a strong correlation between the ultrasound divergence of the stimulated and voluntary motions.

Visual inspection of the source ultrasound videos shows the maximum of the divergence corresponds well to the center of muscle contractions. However, in multiple cases the calculated

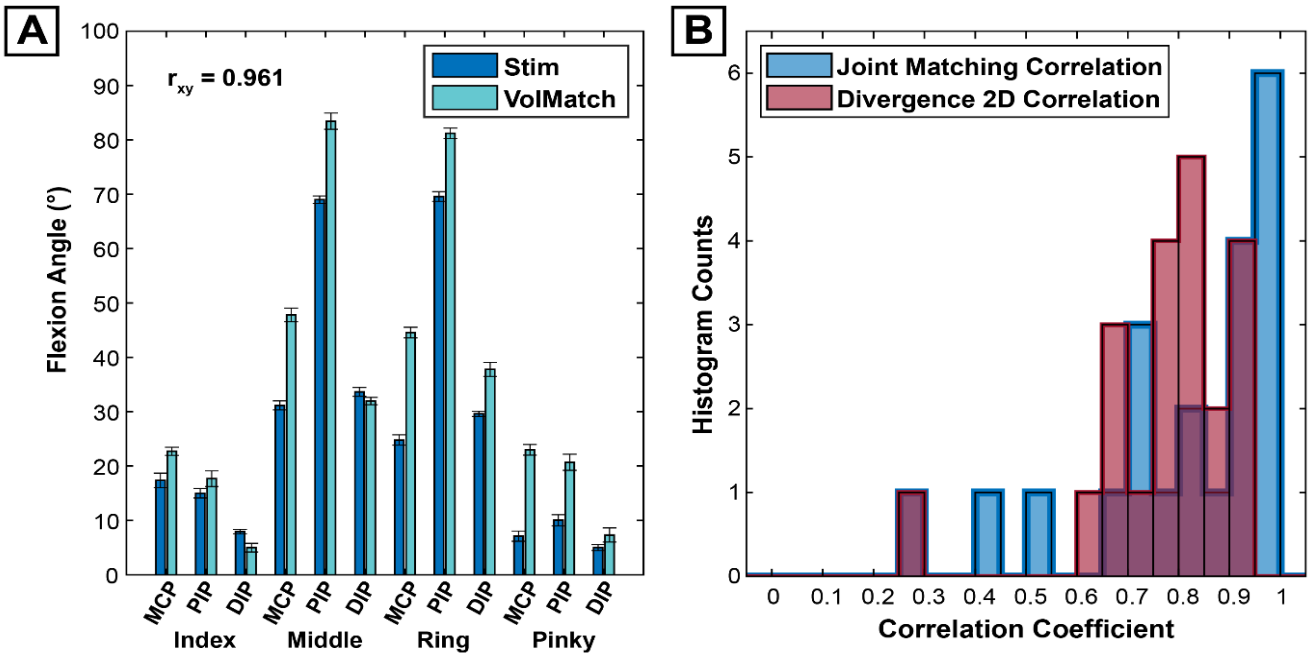

Figure 4: Correlations between Stimulated and Voluntary Matched Motions. A) Sample Joint Motion Correlation between stimulated and Voluntary-Matched data. The colored bars indicate the average angular displacement of each joint across all flexion events, and the error bars indicate the standard error of each set of displacements. The shown rxy value is the sample correlation coefficient. B) Correlation Histogram of Joint Kinematic Matching and Divergence 2D Maps. Blue bars represent the correlation coefficients from all the paired kinematic comparisons of all motion patterns and subjects. Red bars represent the 2D correlation coefficients between the divergence heat maps of the pairs of stimulated and voluntary ultrasound.

III. Results

Among the participants, one subject's motion capture data was irresolvable due to extensive missing marker positions and was therefore excluded from further analysis. At least two distinct stimulated motions were then obtained from the remaining subjects (11 of 12). Of the subjects for whom at least 2 stimulated motions were recorded, at least one proximal and one distal motion was found. Only dual motions involving both the proximal and distal joints were found in 2 subjects, and an additional 4 subjects also had dual joint

divergence resulted in two distinct local maxima, which corresponded to cases where both the FDS and FDP were contracting in similar amounts. For example, the second row of Figure 3 (labeled Index – Distal) shows qualitatively similar regions of red shaded regions of divergence but mismatched absolute maximum locations. To better evaluate all regions of muscle contraction present in the divergence maps, the coordinate locations of the second largest local maxima within 50% of the first largest maximum value were extracted (n=8).

Lastly, as an overview of all the stimulated ultrasound motions across all subjects, a histogram of the depth of all divergence maxima was used to visualize the distribution of

This article has been accepted for publication in a future issue of this journal, but has not been fully edited. Content may change prior to final publication. Citation information: DOI 10.1109/JBHI.2020.3041669, IEEE Journal of Biomedical and Health Informatics

stimulated muscle contractions (Figure 5A). The depth of the tissue movement was used to differentiate between the FDS and FDP muscles during finger flexion. As previously described, some of the divergence maps contained two maxima corresponding to the contraction of both the FDS and FDP muscles, and the dual maxima are shown as dark gray bars, and those only had a single maximum are shown in green/yellow. In addition to the count of divergences within each bin depth, the colors of the bars also indicate the P:D difference of the different joint motions. Figure 5A shows that the motions with a P:D Difference > 0 (Green) was shallower due to the greater activation of the FDS muscle for PIP movement. Conversely, motions with a P:D Difference < 0 (yellow) had a deeper divergence maximum location due to more FDP activation for DIP movement. For further statistical analysis, this distribution of depths was calculated to have a different statistic of 0.083, and a p-value of 0.091. This suggests that the distribution of maximum divergence depths is non-unimodal with marginal significance ($0.1 > p > 0.05$). In general, this bimodal distribution of divergence depths supports the presence of two separately stimulated muscles.

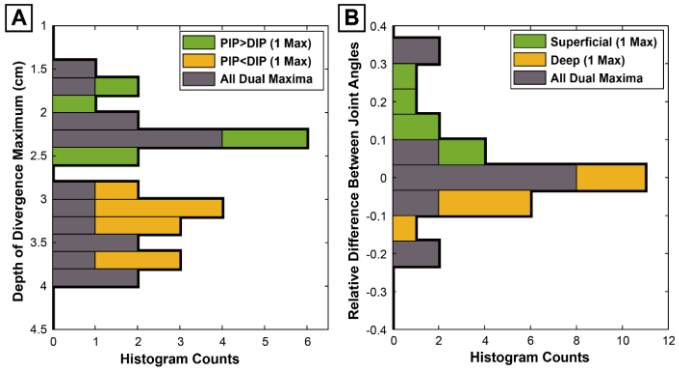

Figure 5: Histogram of Ultrasound Divergence Depths and Relative Joint Differences. A) The depth, or y-axis location, of the divergence maxima of all stimulated motions were included to show the distribution of contraction locations. Green and yellow bars indicate movement sets which had a single divergence maximum, and the gray bars indicates counts where two maxima were present. The y-axis direction has been reversed so that the histogram bar locations corresponds to the depth of the ultrasound with the skin layer at the top B) The relative difference between the displacement of the PIP and DIP of all stimulated motions were included to show the distribution of kinematic patterns. Green and yellow represent the same single maximum trials from (A), and the gray bars similarly represent the same dual maxima trials.

A different analysis of the distribution of the relative PIP and DIP angle displacement differences is shown in Figure 5B. The same data from Figure 5A was re-binned based on relative P:D difference, which represents the overall kinematic pattern. Single divergence motions were labeled as either superficial or deep based on the depth of the divergence relative to the two modes. As these motions were already well separated, all the single divergence motions with a positive P:D difference were also superficial, and vice versa. The gray bars again indicate the movements with dual local maxima, and these movements notably clustered very closely to 0 (aside from two outliers), which indicated a relative similar level of motion of the PIP and DIP joints. Additionally, the distribution of the relative differences showed a much wider positive tail, which suggested that more distal joint movements were more likely to be coupled with DIP and PIP motions. Overall, the two distinct muscle contraction locations showed that the stimulation can activate both superficial and deep flexor muscles.

We also quantified the distribution of electrodes in the stimulation grid. The stimulation sets that induced mainly PIP (proximal), DIP (distal), and dual-joint motions of 6 subjects (the distribution data of the remaining 5 subjects were missing) are illustrated in Figure 6. We did not observe consistent electrode pairs that elicited a particular motion. There were also no distinct distribution patterns for a given motion type.

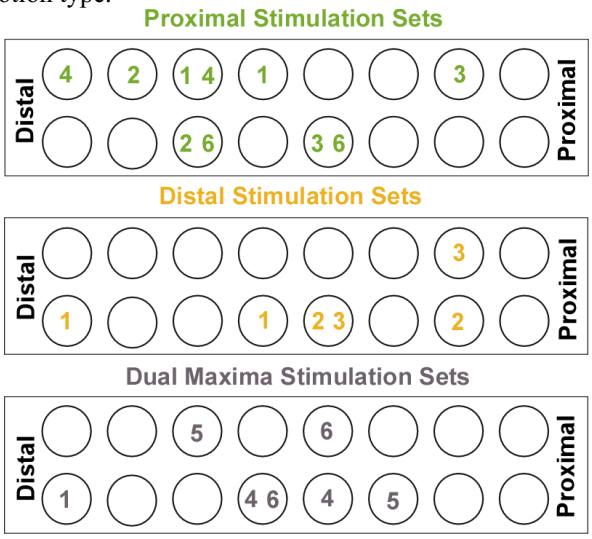

Figure 6: Electrode distribution of six participants. The electrode pairs that elicited different types of motions are identified by the subject number. Left corresponds to the distal side and right corresponds to the proximal side of the upper arm.

IV. Discussion

In the current study, transverse ultrasound was used to quantify the contraction of finger flexor muscles elicited by electrical stimulation of the ulnar and median nerve bundles. The divergence of the ultrasound image deformation was calculated to quantify the contraction of the muscle tissue at different depths. Our results demonstrated that across a variety of stimulated finger flexion motions, elicited muscle contraction in the ultrasound images coincided with two distinct tissue depths. This corresponds to the expected activation of the FDS and FDP muscles which control the PIP and DIP joints, respectively. Evidence of the activation of both superficial and deep finger flexor muscles confirms the increased functional utility of the nerve-bundle stimulation method. The activation of both muscles, concurrently or separately, can help improve joint coordination during electrical stimulation and can also elucidates possible mechanisms of observed delays in muscle fatigue when utilizing nerve stimulation.

A. Ultrasound Imaging for Muscle Activation Detection

Transverse ultrasound was chosen for its ability to distinguish between different regions of tissue movement which was necessary to identify the locations of muscle contraction during finger flexion. Preliminary testing with intramuscular EMG recordings showed that muscle activation does correspond to the contraction of the transverse muscle ultrasound [28]. Various other studies have also utilized ultrasound to classify finger motions. For example, Akhlaghi et al. correlated the pixel-wise differences in the changing ultrasound images during movement to classify finger motions [33]. Huang et al. also utilized feature extraction techniques on ultrasound to identify finger motions [34]. Like other methods of finger motion detection using ultrasound, these approaches do not explicitly identify the exact location of the muscles in each image, as their black-box approach was to classify the finger motion itself. However, as the main purpose of our study was to specifically identify which muscles were contracting due to electrical stimulation, a different approach was used to localize the regions of muscle contraction. As the deformation field itself represents the "flow" or movement of individual pixels between the moving image and its fixed reference, it follows that the divergence of the vector field represents the sources and sinks of the most deformation. With respect to muscles in ultrasound image, these sources correspond to the cross-sectional regions of muscle which show an expansion due to concentric muscle contraction.

The divergence maps of the stimulated and matched-voluntary motions showed that the regions of tissue movement are highly correlated between these two conditions (Figure 4B). One interpretation is that the two kinematically matched movements originate from the same muscle contractions. The various finger flexion patterns elicited by the electrical stimulation activates different sets of muscles, and when voluntarily matching the flexion movement patterns, the subjects recruit similar sets of muscles. Although this seems obvious from a biomechanics standpoint and function of skeletal muscle, in the case of the electrical stimulation, it has only so far been assumed that the same functional set of muscles was activated for a specific movement. Additionally, the matched divergence lends support to the use of the deformation and divergence to quantify muscle contraction. Voluntary motion must be functionally paired with corresponding voluntary muscle contraction, and therefore the changes seen in the ultrasound must also correspond to morphological or structural changes in specific muscles and not simply passive movement due to movement of connective tissues. Subsequently, as these motions are kinematically matched with each original stimulated motion (Figure 4), the resultant similarity of the divergence also supports the conclusion that the divergence indicated active contraction of muscle tissue rather than just passive movement of connective tissues or other muscles.

B. Muscle Activation via Functional Electrical Stimulation

Conventional FES for finger flexion places electrode over the muscles in the forearm to produce desired movements. However, the more superficial FDS muscle, which controls the PIP joint, is much more easily accessible from surface stimulation than the deeper FDP muscle, which controls the DIP joint [9], [12]. An alternative way to activate the deeper FDP muscle involves more invasive percutaneous stimulation methods [35]. In the current study, stimulation of the median and ulnar nerve bundles proximal to the elbow elicits motions which can involve either more proximal or more distal joint flexions. The bimodal distribution of muscle activation depths shown in Figure 5 strongly supports our hypothesis that the stimulation can independently activate both the FDS and FDP muscles. Compared to conventional FES methods, stimulation of the proximal nerve bundles targets a number of nerve fibers before they branch into separate muscles, and therefore can activate multiple sets of muscles from a single electrode pair.

The activation of both FDS and FDP muscles through electrical stimulation is significant for several reasons. First, activation of both muscles enables a more coordinated movement of the PIP and DIP joints, which allows for a more natural flexion of the fingers when holding objects [36]. Second, the shared muscle activity also contributes to grip force across multiple joint levels, such that the load is shared among the muscles, including intrinsic muscles [20]. When larger forces are required, this total activation of the hand muscles through proximal nerve stimulation may provide a much larger grip strength when compared to conventional FES methods. Finally, a previous study using the proximal stimulation method has also shown that when compared to a conventional FES, the proximal stimulation significantly reduced the amount of force decline over prolonged stimulation of the muscles [20], [37], [38]. For smaller repeated motions, the shared activation of multiple muscles could lower the force burden on any single muscle and result in a reduced rate of force decline due to muscle fatigue. Overall, the ability to activate multiple muscles increases the utility of proximal nerve stimulations.

C. Limitations

The use of only the maximum positive divergence was chosen based on preliminary testing and visual inspection of the ultrasound images. However, it is possible that for different locations along the forearm or for some subjects the negative divergence, or convergence, location could be more accurate. Depending on the compartment anatomy of the FDS and FDP, the cross-sectional region of skeletal muscle could either expand concentrically or be pulled out of plane and appear to shrink inward. Further work on the use of ultrasound divergence to quantify cross-sectional changes in skeletal muscle contraction is necessary to fully validate the current methodology.

V. Conclusions

This study investigated whether non-invasive proximal nerve-bundle stimulation can activate both the superficial and deep extrinsic flexor muscles in the forearm. The stimulation was able to elicit motions of the proximal and/or distal joints of different fingers across all subjects, which demonstrated a

distinct bimodal separation of muscle contraction depth. These results support the diverse utility of the proximal nerve stimulation method in eliciting more natural grasp patterns with coordinated multi-joint movements. This may lead to better functional outcomes when used as a rehabilitative tool by training multiple muscles and by also decreasing the fatiguability of the stimulation. Future FES systems utilizing the proximal nerve stimulation method could enable prolonged use and better finger grasp than conventional approaches.

REFERENCES

[1] U. Sveen, E. Bautz-Holter, K. M. Sødring, T. B. Wyller, and K. Laake, "Association between impairments, self-care ability and social activities 1 year after stroke," *Disabil. Rehabil.*, vol. 21, no. 8, pp. 372–377, 1999, doi: 10.1080/096382899297477.

[2] G. J. Snoek, M. J. Ijzerman, H. J. Hermens, D. Maxwell, and F. Biering-Sorensen, "Survey of the needs of patients with spinal cord injury: Impact and priority for improvement in hand function in tetraplegics," *Spinal Cord*, vol. 42, no. 9, pp. 526–532, 2004, doi: 10.1038/sj.sc.3101638.

[3] P. H. Peckham and J. S. Knutson, "Functional Electrical Stimulation for Neuromuscular Applications*," *Annu. Rev. Biomed. Eng.*, vol. 7, pp. 327–360, 2005, doi: 10.1146/annurev.bioeng.6.040803.140103.

[4] F. Quandt and F. C. Hummel, "The influence of functional electrical stimulation on hand motor recovery in stroke patients: a review.," *Exp. Transl. Stroke Med.*, vol. 6, no. 1, p. 9, 2014, doi: 10.1186/2040-7378-6-9.

[5] B. M. Doucet, A. Lam, and L. Griffin, "Neuromuscular electrical stimulation for skeletal muscle function.," *Yale J. Biol. Med.*, vol. 85, no. 2, pp. 201–15, Jun. 2012.

[6] D. B. Popović, "Advances in functional electrical stimulation (FES)," *J. Electromyogr. Kinesiol.*, vol. 24, no. 6, pp. 795–802, 2014, doi: 10.1016/j.jelekin.2014.09.008.

[7] M. Vanderthommen, J. C. Depresseux, L. Dauchat, C. Degueldre, J. L. Croisier, and J. M. Crielaard, "Spatial distribution of blood flow in electrically stimulated human muscle: A positron emission tomography study," *Muscle and Nerve*, vol. 23, no. 4, pp. 482–489, 2000, doi: 10.1002/(SICI)1097-4598(200004)23:4<482::AID-MUS5>3.0.CO;2-I.

[8] D. Farina, A. Blanchietti, M. Pozzo, and R. Merletti, "M-wave properties during progressive motor unit activation by transcutaneous stimulation," *J. Appl. Physiol.*, vol. 97, no. 2, pp. 545–555, 2004, doi: 10.1152/japplphysiol.00064.2004.

[9] N. Filipovic, A. Peulic, N. Zdrakovic, V. Grbovic-Markovic, and A. Jurisic-Skevin, "Transient finite element modeling of functional electrical stimulation," *Gen. Physiol. Biophys.*, vol. 30, no. 1, pp. 59–65, 2011, doi: 10.4149/gpb_2011_01_59.

[10] A. D. Nimbarte, R. Kaz, and Z. M. Li, "Finger joint motion generated by individual extrinsic muscles: A cadaveric study," *J. Orthop. Surg. Res.*, vol. 3, no. 1, pp. 1–7, 2008, doi: 10.1186/1749-799X-3-27.

[11] R. T. Lauer, K. L. Kilgore, P. H. Peckham, N. Bhadra, and M. W. Keith, "The function of the finger intrinsic muscles in response to electrical stimulation.," *IEEE Trans. Rehabil. Eng.*, vol. 7, no. 1, pp. 19–26, Mar. 1999.

[12] X. Bao, Y. Zhou, Y. Wang, J. Zhang, X. Lü, and Z. Wang, "Electrode placement on the forearm for selective stimulation of finger extension/ flexion," *PLoS One*, vol. 13, no. 1, pp. 1–22, 2018, doi: 10.1371/journal.pone.0190936.

[13] M. A. Frankel, V. J. Mathews, G. A. Clark, R. A. Normann, and S. G. Meek, "Control of dynamic limb motion using fatigue-resistant asynchronous intrafascicular multi-electrode stimulation," *Front. Neurosci.*, vol. 10, no. SEP, pp. 1–12, 2016, doi: 10.3389/fnins.2016.00414.

[14] R. a Normann *et al.*, "Coordinated, multi-joint, fatigue-resistant feline stance produced with intrafascicular hind limb nerve stimulation," *J. Neural Eng.*, vol. 9, p. 026019, 2012, doi: 10.1088/1741-2560/9/2/026019.

[15] A. J. Bergquist, J. M. Clair, and D. F. Collins, "Motor unit recruitment when neuromuscular electrical stimulation is applied over a nerve trunk compared with a muscle belly: triceps surae," *J. Appl. Physiol.*, vol. 110, no. 3, pp. 627–637, 2011, doi: 10.1152/japplphysiol.01103.2010.

[16] A. J. Bergquist, M. J. Wiest, and D. F. Collins, "Motor unit recruitment when neuromuscular electrical stimulation is applied over a nerve trunk compared with a muscle belly: quadriceps femoris.," *J. Appl. Physiol.*, vol. 113, no. 1, pp. 78–89, Jul. 2012, doi: 10.1152/japplphysiol.00074.2011.

[17] H. Shin, Z. Watkins, and X. Hu, "Exploration of Hand Grasp Patterns Elicitable Through Non-Invasive Proximal Nerve Stimulation," *Sci. Rep.*, vol. 7, no. 1, p. 16595, 2017, doi: 10.1038/s41598-017-16824-1.

[18] H. Shin and X. Hu, "Flexibility of Finger Activation Patterns Elicited through Non-invasive Multi-Electrode Nerve Stimulation," *Annu. Int. Conf. IEEE Eng. Med. Biol. Soc.*, vol. 2018, pp. 1428–1431, 2018, doi: 10.0/Linux-x86_64.

[19] Y. Zheng and X. Hu, "Improved muscle activation using proximal nerve stimulation with subthreshold current pulses at kilohertz-frequency," *J. Neural Eng.*, vol. 15, no. 4, p. 046001, Aug. 2018, doi: 10.1088/1741-2552/aab90f.

[20] H. Shin, R. Chen, and X. Hu, "Delayed fatigue in finger flexion forces through transcutaneous nerve stimulation," *J. Neural Eng.*, vol. 15, no. 6, p. 066005, Dec. 2018, doi: 10.1088/1741-2552/aadd1b.

[21] C. J. De Luca, "The use of surface electromyography in biomechanics," *J. Appl. Biomech.*, vol. 13, no. 2, pp. 135–163, May 1997, doi: 10.1123/jab.13.2.135.

[22] R. Merletti and A. Farina, "Analysis of Intramuscular electromyogram signals," *Philos. Trans. R. Soc. A Math. Phys. Eng. Sci.*, vol. 367, no. 1887, pp. 357–368, 2009, doi: 10.1098/rsta.2008.0235.

[23] M. D. Crema, A. F. Yamada, A. Guermazi, F. W. Roemer, and A. Y. Skaf, "Imaging techniques for muscle injury in sports medicine and clinical relevance," *Curr. Rev. Musculoskelet. Med.*, vol. 8, no. 2, pp. 154–161, 2015, doi: 10.1007/s12178-015-9260-4.

[24] D. W. Goodwin, "Imaging of Skeletal Muscle," *Rheum. Dis. Clin. North Am.*, vol. 37, no. 2, pp. 245–251, 2011, doi: 10.1016/j.rdc.2011.01.007.

[25] S. Sikdar, Q. Wei, and N. Cortes, "Dynamic ultrasound imaging applications to quantify musculoskeletal function," *Exerc. Sport Sci. Rev.*, vol. 42, no. 3, pp. 126–135, 2014, doi: 10.1249/JES.0000000000000015.

[26] J. Shi, J. Y. Guo, S. X. Hu, and Y. P. Zheng, "Recognition of Finger Flexion Motion from Ultrasound Image: A Feasibility Study," *Ultrasound Med. Biol.*, vol. 38, no. 10, pp. 1695–1704, 2012, doi: 10.1016/j.ultrasmedbio.2012.04.021.

[27] Y. P. Zheng, M. M. F. Chan, J. Shi, X. Chen, and Q. H. Huang, "Sonomyography: Monitoring morphological changes of forearm muscles in actions with the feasibility for the control of powered prosthesis," *Med. Eng. Phys.*, vol. 28, no. 5, pp. 405–415, 2006, doi: 10.1016/j.medengphy.2005.07.012.

[28] Y. Zheng, H. Shin, D. G. Kamper, and X. Hu, "Automatic Detection of Contracting Muscle Regions via the Deformation Field of Transverse Ultrasound Images: A Feasibility Study," *Ann. Biomed. Eng.*, 2020, doi: 10.1007/s10439-020-02557-2.

[29] H. Shin, Y. Zheng, and X. Hu, "Variation of Finger Activation Patterns Post-stroke Through Non-invasive Nerve Stimulation," *Front. Neurol.*, vol. 9, no. December, pp. 1428–1431, Dec. 2018, doi: 10.3389/fneur.2018.01101.

[30] H. Shin and X. Hu, "Multichannel Nerve Stimulation for Diverse Activation of Finger Flexors," *IEEE Trans. Neural Syst. Rehabil. Eng.*, 2019, doi: 10.1109/TNSRE.2019.2947785.

[31] J.-P. Thirion, "Image matching as a diffusion process: an analogy with Maxwell's demons," *Med. Image Anal.*, vol. 2, no. 3, pp. 243–260, Sep. 1998, doi: 10.1016/S1361-8415(98)80022-4.

[32] T. Vercauteren, X. Pennec, A. Perchant, and N. Ayache, "Diffeomorphic demons: efficient non-parametric image registration.," *Neuroimage*, vol. 45, no. 1 Suppl, pp. S61-72, Mar. 2009, doi: 10.1016/j.neuroimage.2008.10.040.

[33] N. Akhlaghi *et al.*, "Real-time classification of hand motions using ultrasound imaging of forearm muscles," *IEEE Trans. Biomed. Eng.*, vol. 63, no. 8, pp. 1687–1698, 2016, doi: 10.1109/TBME.2015.2498124.

[34] Y. Huang, X. Yang, Y. Li, D. Zhou, K. He, and H. Liu, "Ultrasound-Based Sensing Models for Finger Motion Classification," *IEEE J. Biomed. Heal. Informatics*, vol. 22, no. 5,

pp. 1395–1405, 2018, doi: 10.1109/JBHI.2017.2766249.

[35] M. R. Popovic, D. B. Popovic, and T. Keller, "Neuroprostheses for grasping," *Neurol. Res.*, vol. 24, no. 5, pp. 443–452, 2002, doi: 10.1179/016164102101200311.

[36] U. Arnet, D. A. Muzykewicz, J. Fridén, and R. L. Lieber, "Intrinsic hand muscle function, part 1: Creating a functional grasp," *J. Hand Surg. Am.*, vol. 38, no. 11, pp. 2093–2099, 2013, doi: 10.1016/j.jhsa.2013.08.099.

[37] Y. Zheng, H. Shin, and X. Hu, "Muscle Fatigue Post-stroke Elicited From Kilohertz-Frequency Subthreshold Nerve Stimulation," *Front. Neurol.*, 2018, doi: 10.3389/fneur.2018.01061.

[38] Y. Zheng and X. Hu, "Reduced muscle fatigue using kilohertz-frequency subthreshold stimulation of the proximal nerve," *J. Neural Eng.*, 2018, doi: 10.1088/1741-2552/aadecc.